Comparative Cytotoxic and Anticancer Effect of Taxol Derived from *Aspergillus terreus* and *Taxus brevifolia*

[1]Nabila Zein and [2]Ashraf S. El-Sayed
[1]*Department of Chemistry Biochemistry Division, Faculty of Science,*
[2]*Department of Microbiology and Botany, Faculty of Science, Zagazig University, Zagazig, Egypt*

Abstract: Taxol is a highly oxygenated diterpenoid of broad spectrum anticancer activity, due it unique specificity for binding with tubulin β-subunits heterodimer of tumor cells, disrupting their mitotic division. Taxol has been commercially produced from *Taxus brevifolia*, however, its lower yield, accessibility and pricey are the current challenges for this technology, thus, exploring of fungi as alternative source of taxol could opened new platforms for production of this drug. From our previous studies, taxol has been produced by *A. terreus* with the same chemical structural identity with that from *T. brevifolia*. Thus, the objective of this study was to comparatively evaluate the cytotoxicity and anticancer activity of *Aspergillus Terreus* taxol (AT-taxol) and commercial *Taxus Brevifolia* taxol (TB-taxol) against ehrlich ascites carcinoma in female Swiss albino mice via. intraperitoneal injection. Taxol from both sources had the same cytotoxic biochemical patterns as well as anticancer activity against ehrlich ascites carcinoma. Positive control mice showed an increasing on the serum Nitric Oxide (NO) and lipid peroxidation (MDA) level accompanied by a decline in Total Antioxidant Capacity (TAC) in addition to MMP9 upregulation and caspase-3 down regulation. Histopathologically, liver and kidney tissues showed some pathological features due to the oxidative stress induced by EAC. AT-taxol and TB-taxol gave the same potent antioxidant and anticancer properties by augmenting the antioxidant defense system through induction of apoptosis and protecting both liver and kidney against oxidative stress induced by ehrlich ascites carcinoma.

Corresponding Author:
Nabila Zein
Department of Chemistry Biochemistry Division, Faculty of Science, Zagazig University, Zagazig, Egypt

INTRODUCTION

Taxol is the common anticancer drug for treatment of various types of cancers; gastric, breast, lung and ovarian[1] by stabilizing their polymerized microtubules resulting in arrest of G0/G1 and G2/M cell cycle [2]. In chronic ovarian cancer that may leads to malignant ascites, taxol treatment displayed a good therapeutic response, so, the intraperitoneal regime of taxol has been considered as an efficient remedy for peritoneal

metastasis[3]. Taxol has been approved by the US National Cancer Institute in 2014 as a recommended regimen for treatment of ovarian cancer with peritoneal metastasis.

Taxol is one of the well-known natural anticancer agent obtained from the bark of *Taxus brevifolia* it has been used frequently against various types of tumor cells. However, the yield of this compound is very tiny, for example to obtain 1 gm of taxol it does needs about 8-10 kg of the plant bark which could be obtained from 3-5 trees of *T. brevifolia*, in addition to the fluctuation and vulnerability of the plant growth and their taxol yield with the unpredictable environmental and ecological conditions[4, 5]. Alternatives, potency of some endophytic for taxol production raise the hope for industrial production of taxol, increasing its accessibility, especially with the feasibility of genetic manipulation of fungi and their fermentation process, low cost process, independence on climatic changes, short life span and bulk fermentation conditions as reviewed by El-Sayed *et al.*[6]. Various endophytes from medicinal plants with the metabolic potency for taxol production have been reviewed[6]. Recently has been purified and chemically characterized from *Aspergillus terreus*, an endophyte of *P. gracilior*[7], however, the biological functionality and cytotoxicity in vivo has not been characterized yet, comparing to commercial taxol.

Thus, the objective of this research was to comparatively fulfil the cytotoxic and anticancer activity of taxol extracted from *A. terreus* with the commercial taxol of *T. brevifolia in vivo*, using experimental mice infected with EAC cells.

MATERIALS AND METHODS

Fungal isolates and culture conditions: *Aspergillus terreus* EFB108 was selected among the recovered endophytic fungal isolates inhabiting podocarpus gracilior as the highest taxol producer[7]. The fungal isolate was morphologically, molecularly identified and deposited into the genbank with accession number MF377552. The fungal isolate was grown on MID medium that contains 0.5 g yeast extract, 0.02 g $N_aH_2PO_4$. H_2O, 0.005 g $MnSO_4$, 0.2 g C_a $(NO_3)2$, 30 g sucrose, 0.06 g KCl, 5.0 g ammonium tartrate, 1.0 g soytone, 0.08 g KNO_3, 0.36g $MgSO_4$, 0.014 g H_3BO_3, 0.002 g $FeCl_3$, 0.003 g $ZnSO_4$. $7H_2O$ and 0.014 g KI, dissolved in 1 L distilled water. The fungal spores (6 days old) were inoculated into 250 mL media/L erlenmeyer flask then cultures incubated for 21 days at 30°C. Blanks of the same media free of fungal spores were maintained at the same conditions. After incubation, the fungal mycelia were removed by filtration and the filtrates were amended with 0.2 g of sodium bicarbonate to precipitate fatty acids. Taxol was extracted with dichloromethane and the organic phase was collected, evaporated to dryness then residues were re-dissolved in methanol. Taxol was checked by TLC and quantified by HPLC chromatographic analyses[8].

Taxol purification, quantification and chemical identification: The extracted taxol samples were fractionated using silica gel plates (MerkKgaA 60 F254, Germany) with the developing solvent system dichloromethane/methanol/dimethylformamide (90:9:1, v/v/v). After running, the taxol spots were visualized by illumination of the plate at λ254 nm, giving blue colored spots comparing to authentic taxol (Sigma Aldrich Cat. # T7402). The purity and concentration of taxol were checked by HPLC of reverse column C18 column (Eclipse plus C18 4.6×150 mm, agilent technol.) Using mobile phase acetonitrile/water (52:48 v/v) at flow rate 1.0 mL/min, each sample was analyzed for 20 min. The fractions were scanned from 200-500 nm by photodiode array detector. The chemical identity and concentration of taxol were confirmed from the retention time and absorption peak area at 228 nm comparing to authentic one. The chemical structure of extracted taxol was confirmed from the proton and carbon NMR spectra using JEOL (ECA-500II) 500 MHz NMR at Faculty of Science, Mansoura University, Egypt. The sample was dissolved in CDCl3 prior analysis. The chemical shifts and coupling constants are expressed in part per million (d-scale) and Hertz (Hz), respectively.

Experimental animals and taxol sources: A total 40 adult female Swiss albino mice at 8 weeks of age, their weight ranging from 20-25 g from the same bred were obtained from the National Cancer Institute, Cairo University, Egypt. Ehrlich ascites carcinoma cells were kindly obtained from the National Cancer Institute, Cairo University, Egypt, maintained by serial intraperitoneal transplantation of 2.5×106 cells/0.3 mL in female Swiss albino mice[9]. Commercial taxol was purchased from Bristol-Myers Squibb Inc. (Princeton, NJ, USA).

Experimental design: The 40 female Swiss albino mice were distributed into 4 different groups, 10 mice per group. Group 1; negative control mice injected ip. with 0.3 mL saline. Group 2; positive control mice injected ip. with EAC cells at concentration of 2.5×106 cells /0.3 mL/mouse at the beginning of experiment. Group 3; positive control mice with EAC cells acclimated for 24 h and injected with 1 mg kg^{-1} BW commercial paclitaxel[2]. Group 4; positive control mice with EAC cells acclimated for 24 h and injected with 1 mg kg^{-1} BW *Aspergillus terreus* taxol. The four experimental groups of mice were acclimated for 5 days at the same physical and nutritional conditions. Then, the mice were euthanized by CO_2 exposure followed by cervical dislocation according to Institutional Animal Care and Use Committee (IACUC) and the following biochemical and histological analyses were conducted.

Blood sampling: Samples of blood for biochemical analyses were collected in plain tubes, centrifuged at 4000 rpm for 15 min and the serum was collected and

stored at -20°C till use. Whereas blood samples for estimating hematological parameters were collected in EDTA containing tubes and analyzed with the automatic CBC analyzer (SesmexKx-21). EAC cells were collected and divided into 2 tubes containing heparinized saline to prevent its clotting, one of them for estimating the markers of apoptosis and the other for the cytomorphological studies.

Biochemical parameters analysis: Malondialdehyde (MDA)[10], Nitric Oxide (NO)[11] and Total Antioxidant Capacity (TAC)[12] biomarkers in the serum were estimated using Biodiagnostic kits (Biodiagnostic Company, Giza/Egypt).

Apoptosis markers: The activities of caspase-3[13] and MMP-9[14] of EAC cells were determined using the standard assays kits according to the manufacturer's protocol (Enzo Life Sciences, Inc.).

Histopathological study: Specimens of liver and kidney tissues have been fixed with 10% buffered neutral formalin, paraffin sections cut into 5 μm thickness, stained with haematoxylin and eosin and later examined by light microscope.

Cytomorphological study: Cytomorphological analysis of EAC cells was conducted using Giemsa stains as described by Rahman *et al.*[15] using a smear of EAC cells.

Statistical analysis: Statistical analysis of the data using one way of variance by SPSS 14.0 Version[16], expressed by mean±SD and p-values <0.05 were considered as statistically significant.

Ethics statement: The animal experiments were conducted according to the guidelines of Institutional Animal Care and Use Committee (IACUC) at Faculty of Medicine, Zagazig University and confirmed to follow NIH guidelines under protocol 15-08-263.

RESULTS AND DISCUSSION

Extraction and chemical identification of *Aspergillus terreus* taxol: *Aspergillus terreus* was grown on MID medium for 21 days at 30°C, then taxol was extracted by dichloromethane and the residues were dissolved in methanol. The crude compounds were fractionated by TLC and the spots with the same R_f value of authentic taxol were scraped off from the silica plates and their purity and concentration were determined by HPLC (Fig. 1).

The yield of taxol by *A. terreus* was 20.2 μg/g fungal dry weight. The chemical structure of extracted taxol was verified from the HNMR spectra compared to authentic sample. From the results (Fig. 1), the purified taxol from *A. terreus* has the same chemical identity with the authentic one. To validate the functionality and cytotoxicity of taxol extracted from *A. terreus*, the in vivo biochemical analysis using experimental animals as well as their anticancer activity against EAC were studied.

Biochemical and hematological parameters analysis: The biochemical parameters of mice in response to transfection with EAC cells and treatment with *A. Terreus* taxol (AT-taxol) and commercial taxol of *Taxus Brevifolia* (TB-taxol) were assessed. From the results (Table 1) an overall increase on the titer of MDA and NO by about 6 folds and 2 folds, respectively, of positive control mice
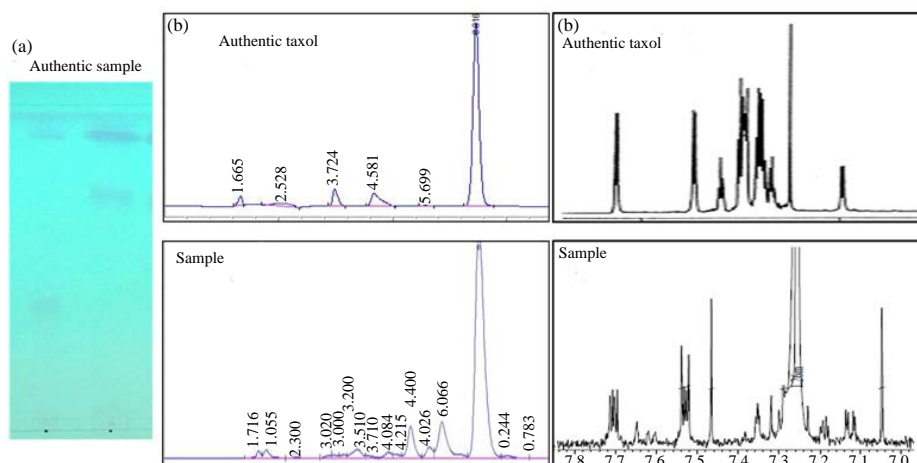

Fig. 1(a-c): Chemical identity of *A. terreus* extracted taxol. The fungal cultures were grown on MID medium, incubated for 20 days, the cultures were filtered and taxol was extracted by the standard protocol as described in materials and methods. The chemical identity of taxol extracted from *A. terreus* was confirmed from the TLC chromatogram, (a) HPLC chromatogram, (b) From HNMR chromatogram and (c) Comparing to the authentic taxol

Table 1: *In vivo* biochemical parameters of mice injected with EAC cells in response to fungal taxol (AT-taxol) and commercial taxol (TB-taxol)

Parameters	MDA (nmol mL^{-1})	NO (µmol mL^{-1})	TAC (mmol L^{-1})
Negative control	31.4±14.5	41.9±9.4	3.20±0.74
Positive control	182.7±35.4[*a]	79.2±4.5[*a]	1.46±0.39
AT-taxol	49.4±4.8[*b]	49.8±4.2[*b]	2.68[*b]±0.37
TB-taxol	61.9±4.9[*b]	60.9±1.8[*b]	2.91[*b]±0.29

Values are expressed as mean±SE: a: Values significantly differ from negative control group; b: Values significantly differ from positive control group; *: p<0.001

Table 2: Hematological parameters of mice injected with EAC cells in response to AT-taxol and TB-taxol

Parameters	RBC (X106)	Hb (g/dl)	WBC (X10^3)	PLT(X10^3)
Negative control	7.7±1.1	14.3±1.1	9.1±0.75	165.9±16
Positive control	5.7±0.5[*a]	11.1±1.6[*a]	6.1±0.7[*a]	116.7±11.5[*a]
AT-taxol	7.3±0.9[*b]	14.7±1.3[*b]	9.2±0.7[*b]	140.8±14[*b]
Change (%)	28.07 %	32.4%	50.8%	20.6%
TB-taxol	7.2±0.76[*b]	14.2±1.6[*b]	8.7±0.7[*b]	135±9.9[*b]
Change (%)	26.3 %	27.9%	44.2%	15.6%

Values are expressed as mean±S.E: a: Values significantly differ from negative control group; b: Values significantly differ from positive control group; *p<0.001; Change%: Values different from positive control group

(EAC cells while the titer of TAC was reduced by 2 folds than the negative control mice (normal mice). Upon treatment with AT-taxol and TB-taxol, the titers of MDA, NO and TAC of positive control mice were restored to their approximately normal titers. The NO levels of EAC-mice were reduced by 59.03 and 30.04% in response to AT-taxol and TB-taxol, respectively, also it was observed that MDA level was lowered by 72.9 and 66.1% in serum of positive control mice in response to AT-taxol and TB-taxol, comparing to negative controls. The TAC levels of EAC cells mice were increased by 83.56 and 99.31% in response to AT-taxol and TB-taxol, comparing to negative controls. EAC tumors has been chosen for this comparative study, as it sensitive to chemotherapeutic agents with no regression, high transplantable capability with 100% malignancy and shorter life span, hyperdiploid undifferentiated carcinoma[17]. Nitric oxide plays a vital role in tumor progression as it controlled by the inducible Nitric Oxide Synthase (iNOS) that subsequently promotes the cytokine mediated cell destruction, stimulating the pathogenesis by oxidative stress[18]. EAC have disturbs the function of the macrophages which has been proved by the significant increases on NO serum level in positive control group[19], comparing to negative control. As well as, nitric oxide was reported to reacts with free radicals, producing peroxy-nitrite oxidizing the LDL, leading to irreversible damage to the cell membrane. Significant improvement on in the antioxidant enzymes, oxidative stress markers, nucleic acids content and gene expression accompanied by the reduction of NO levels were determined in response to taxol treatment of positive control mice[20]. Malondialdehyde has been found to be over induced in cancerous tissues more than normal healthy cells, referring to autocatalytic free radical chain reaction and lipid peroxidation[21]. From the obtained results, AT-taxol and TB-taxol significantly decreased the lipid peroxidation that caused by the oxidative damage induced by EAC as shown from the levels of Malondialdehyde (MDA) and Total Antioxidants Capacity (TAC).

From the hematological parameters, the titers of RBC, HB, WBC and PLT were strongly reduced by about 25% in positive control (mice with EAC cells) comparing to negative control mice. Interestingly, upon treatment with AT-taxol and TB-taxol, these hematological parameters restored very closely to be normal range as shown in Table 2. The oxidative injury has been reported to be consistent with the erythrocyte damage, increasing on erythrocyte osmotic fragility that leads to Thrombocytopenia as a marker for monitoring the acute and chronic experimental inflammation. It has been demonstrated that EAC produced pancytopenia as shown by erythrocytopenia, thrombocytopenia and leucocytopenia in the blood as evidenced by the reduction in the RBC, hemoglobin, platelets and total WBC counts. Taxol have significantly reduced the oxidative damage caused by EAC and altered the hematological parameters towards normal range which might be due to activation of antioxidant enzymes through significantly increasing in RBC counts, Hb concentration, platelet counts and WBC comparing to positive group. These results strongly pointed to the similarity on structural identity of taxol from *A. terreus* and *T. brevifolia*.

Apoptosis markers: The parameters of apoptosis as direct indicator for progression of EAC cells in mic such as MMD9 and caspase 3 were determined in response to treatment with taxol from both sources. Normalizing to the positive controls, the titer of MMP9 was reduced by about 50% while the titer of caspase 3 was increased by 2.5 folds upon using AT-taxol and TB-taxol, respectively. Apoptosis, programmed cell death, a physiological process that implemented with removal of damaged harmful cells that distinguish it from necrotic cell death it has many characterized features as chromatin condensation and cell shrinkage that might be occurred in response to oxidative stress, deprivation of growth factors and DNA damage[22]. The apoptotic pathway involved many cysteine-aspartic acid proteases, caspases that inactively present in the cell cytoplasm till activation by
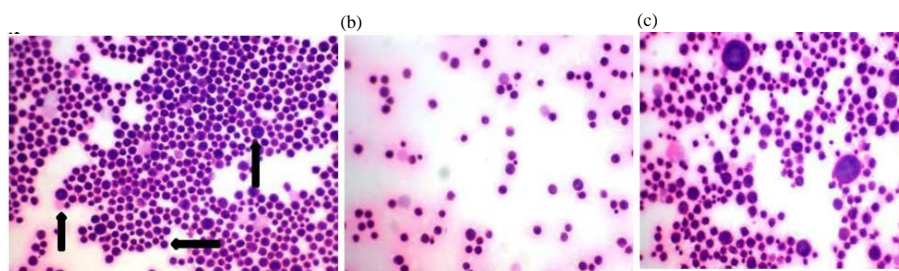
Fig. 2(a-c): Cytomorphological examination of EAC cells (H and Ex400). Positive control group showing large number of variable sized malignant cells, (a) EAC cells treated with AT-taxol, (b) TB-taxol and (c) With significant reduction in number of malignant cells

proteolytically cleavage. Some caspases are initiator proteins for apoptosis as caspase 8 and 9 by activating other caspases leading to proteolysis of certain proteins causing DNA damage as caspase 3 and 7 that causes DNA fragmentation[23]. Caspase 3 is one of the main executioner caspases that modulate apoptosis[24]. Matrix Metalloproteinases (MMP9) are vital contributors to cancer initiation and progression that considered as tumor micro-environment regulators[25]. In breast, lung, colon and pancreatic carcinomas, MMP9 were overexpressed in malignant tissues comparing to adjacent normal tissues[26]. Apoptosis induced in cancerous cells is reflected by downregulation of MMP9 expression and upregulation of caspase 3 expression[27]. From the results, taxol treatment lowered the activity of MMP9 and raised caspase 3 activity, ensuring the cytotoxic activity of taxol against EAC cells. In another study, taxol has been recognized to induces apoptosis in cancerous cells by activating the intrinsic pathway including caspase 3, caspase 8, cytochrome C and BID-mitochondria, downregulating the antiapoptotic factors MMP9, COX-2, Bcl2, inflammatory cytokines and adhesion molecules[28].

Cytomorphological and histopathological studies: The cytomorphological identities of EAC cells in response to treatment with AT-taxol and TB-taxol were illustrated in Fig. 2. Interestingly from the results, large number of variable sized malignant cells (large, medium and small) with pleomorphic hyper chromatic nuclei and eosinophilic cytoplasm were observed in positive controls of EAC cells in contrary to the limited numbers of these malignancies in response to treatment with AT-taxol and TB-taxol (Fig. 2a-c). Apparently, the growth and proliferation of EAC cells treated with AT-taxol and TB-taxol had the same cytological pattern approving the identical chemical structure of taxol from both sources. These results suggested that taxol exhibits a potential antitumor and antioxidant activities in vivo, possessing the apoptosis mechanism[29]. Positive control mice liver showed cellular inflammatory infiltrations, congestion in blood vessels, hyper-chromatinea, nuclear hypertrophy

debris in central vein and haemorrhage with wide sinusoids. The histopathological investigation of mice liver tissue was shown in photomicrograph Fig. 3. The negative control mice showing normal liver tissue formed of hepatic strands with central vein surrounded by rows of polyhedral hepatocytes with eosinophilic cytoplasm and normal buffer cells and blood sinusoids. While the positive control mice liver showing a dilated central vein congested with damaged RBCs and cellular debris surrounded by hepatic lobules separated by dense fibrous bands, heavy aggregation of chronic inflammatory cells and dilated blood sinusoids (Fig. 3b). Overall, the visible changes of liver tissues in response to EAC cells had been partially restored upon treatment taxol from both sources. The liver tissues of mice treated with AT-taxol showing a good organization to the hepatic strands surrounding the normal central vein with more prominent nuclei of hepatocytes and good eosinophilic cytoplasm, however, some of the blood sinusoids are still dilated. Taxol from both sources displaying visible improvements in the hepatic environment, comparing to positive controls, however, some pathological criteria are still present in the form of dilated and congested central vein, blood sinusoids and disorganized hepatic strands. It is well known that existence of tumors at any organ of the experimental animal have negative impacts on liver functions[30] that it is considered the main organ for drug activation, detoxification and other metabolic reactions. Histologically, the liver tissues of mice with tumor cells showing a dilated congested central vein with aggregation of chronic inflammatory cells in contrary to taxol treated mice in which most of the pathological alterations induced by EAC cells in mice were improved. Also, for taxol treated mice, the liver tissue showed a normal appearance to large extent as reflected by normal array of the hepatic cords radiating from the central vein with no appearance of cellular inflammatory infiltration, the cytoplasm is intact and the nuclei that similarly to negative controls.

The histopathological features of the mice kidney tissues were shown in the photomicrograph Fig. 4. The negative control mice showing normal renal tissue formed
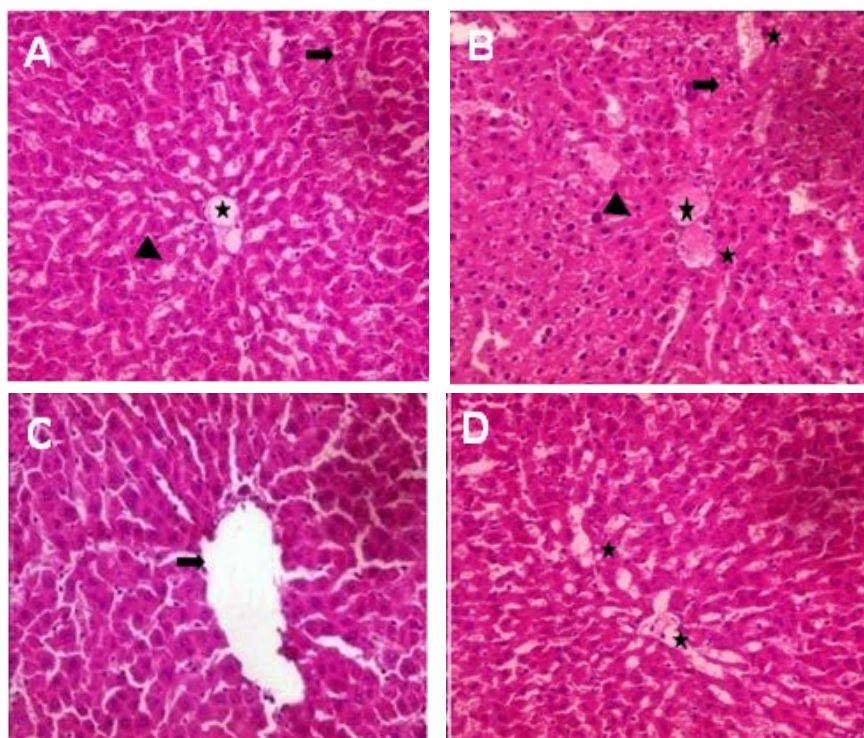
Fig. 3(A-D): Photomicrograph of histopathological investigation of mice liver tissues of negative controls, (A) Positive controls, (B) Treated with commercial TB-taxol, (C) AT-taxol and (D) At magnification 400 X
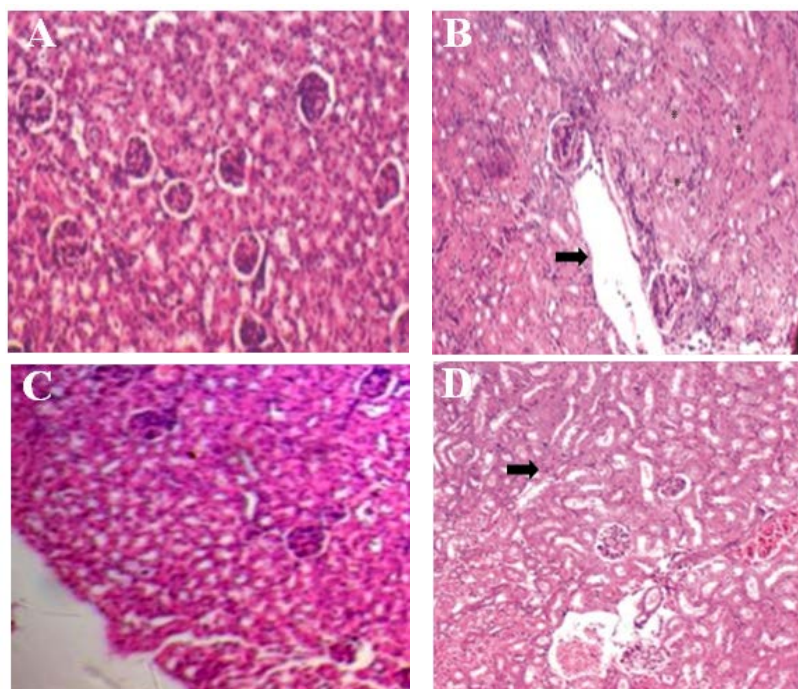

Fig. 4(A-D): Photomicrograph of histopathological examination of kidney tissues in negative control mice, (A) Positive control mice, (B) Treated with AT-taxol, (C) TB-taxol and (D) At magnification X 400

Table 3: Assessment of Apoptosis markers of mice injected with EAC cells in response to AT- taxol and TB-taxol

Parameters	MMP9 (ng mL^{-1})	Caspase 3 (ng mL^{-1})
Positive control	118.6±1.04	28.2±61.18
AT-taxol	62.27±2.57*	79.87±3.4*
Change (%)	47.49%	64.61 %
TB-taxol	61.0±3.7*	79.53±3.19*
Change (%)	48.56%	64.46 %

Values are expressed as mean±SE: *Values significantly differ from positive control group, p<0.001. Change%: Values different from positive control group

of numerous uniform rounded glomeruli and renal tubules lined by intact epithelium with narrow lumina while the positive control mice show a strong damage and sclerotic renal corpuscle with misangeal hemorrhage and adjacent dilated and congested renal vein (Fig. 4b) and (Table 3). The cells of renal tubules exhibited cytoplasmic vacuolization and focal necrosis, leucocytic infiltration. Practically, the positive control tissues treated with taxol showing a strong amelioration in the renal environment with good profile for renal corpuscles and renal tubules, confirming the similarity on biological functionality of taxol from both sources. Taxol treatment displaying an improvement on renal tissues, renal corpuscles and renal tubules with nearly normal lumina, comparing to positive control samples. However, congested renal vein surrounded by renal glomeruli and renal tubules with few aggregates of inflammatory cells was demonstrated. Positive control mice kidney showed dilated congested renal vein surrounded by infiltrated renal glomeruli and renal tubules and aggregation of inflammatory cell. It was obvious that treatment with taxol improves many pathological alterations caused by EAC cells in mice. From the histological investigation of kidney tissues of mice treated with taxol, a strong improvement on the kidney renal tissue was observed with congested renal vein surrounded by renal glomeruli and renal tubules with few aggregates of inflammatory cells. Overall, the kidney tissue showed a normal renal tissue with round uniform renal glomeruli surrounded by normal renal tubules similar to negative controls[31].

CONCLUSION

From this comparative study, taxol from *A. terreus* had the same cytotoxic effect and anticancer activity of commercial *T. brevifolia* taxol as revealed from the biochemical, histological parameters and tumor growth markers. To the best of knowledge, this is the first report describing the cytotoxic and anticancer efficiency of *A. terreus* taxol comparing to commercial *T. brevifolia* taxol, that will emphasize the fungal source as a novel platform for industrial production of taxol production.

REFERENCES

01. Flores, M.L., C. Castilla, R. Avila, M. Ruiz-Borrego, C. Saez and M.A. Japon, 2012. Paclitaxel sensitivity of breast cancer cells requires efficient mitotic arrest and disruption of Bcl-xL/Bak interaction. Breast Cancer Res. Treat., 133: 917-928.
02. Badr El-Din, N.K., D.A. Ali, M. Alaa El-Dein and M. Ghoneum, 2016. Enhancing the apoptotic effect of a low dose of paclitaxel on tumor cells in mice by arabinoxylan rice bran (MGN-3/Biobran). Nutr. Cancer, 68: 1010-1020.
03. Kinoshita, J., S. Fushida, T. Tsukada, K. Oyama and T. Watanabe et al., 2014. Comparative study of the antitumor activity of Nab-paclitaxel and intraperitoneal solvent-based paclitaxel regarding peritoneal metastasis in gastric cancer. Oncol. Rep., 32: 89-96.
04. Wani, M.C., H.L. Taylor, M.E. Wall, P. Coggon and A.T. McPhail, 1971. Plant antitumor agents. VI. The isolation and structure of taxol, a novel antileukemic and antitumor agent from *Taxus brevifolia*. J. Am. Chem. Soc., 93: 2325-2327.
05. Khani, S., J. Barar, A. Movafeghi and Y. Omidi, 2012. Production of Anticancer Secondary Metabolites: Impacts of Bioprocess Engineering. In: Biotechnological Production of Plant Secondary Metabolites, Orhan, I.E. (Ed.). Bentham Science Publishers, Sharjah, United Arab Emirates, ISBN: 978-1-60805-114-4, pp: 215-240.
06. El-Sayed, A.S., S.E. Abdel-Ghany and G.S. Ali, 2017. Genome editing approaches: Manipulating of lovastatin and taxol synthesis of filamentous fungi by CRISPR/Cas9 system. Applied Microbiol. Biotechnol., 101: 3953-3976.
07. El-Sayed, A.S., S. Safan, N.Z. Mohamed, L. Shaban, G.S. Ali and M.Z. Sitohy, 2018. Induction of taxol biosynthesis by Aspergillus terreus, endophyte of Podocarpus gracilior Pilger, upon intimate interaction with the plant endogenous microbes. Process Biochem., 71: 31-40.
08. Li, J.Y., G. Strobel, R. Sidhu, W.M. Hess and E.J. Ford, 1996. Endophytic taxol-producing fungi from bald cypress, Taxodium distichum. Microbiology, 142: 2223-2226.
09. Al-Ghannam, S.M., H.H. Ahmed, N. Zein and F. Zahran, 2013. Antitumor activity of balanitoside extracted from Balanites aegyptiaca fruit. J. Applied Pharm. Sci., 3: 179-191.

10. Satoh, K., 1978. Serum lipid peroxide in Cardio Vascular Disease, determined by a new colorimetric method. Clin. Chim. Acta., 90: 37-43.

11. Montgomery, H.A.C. and J.E. Dymock, 1961. The determination of nitrite in water. Analyst, 86: 414-416.

12. Koracevic, D., G. Koracevic, V. Djordjevic, S. Andrejevic and V. Cosic, 2001. Method for the measurement of antioxidant activity in human fluids. J. Clin. Pathol., 54: 356-361.

13. Casciola-Rosen, L., D.W. Nicholson, T. Chong, K.R. Rowan, N.A. Thornberry, D.K. Miller and A. Rosen, 1996. Apopain/CPP32 cleaves proteins that are essential for cellular repair: A fundamental principle of apoptotic death. Jo. Exp. Med., 183: 1957-1964.

14. McCawley, L.J. and L.M. Matrisian, 2001. Matrix metalloproteinases: They're not just for matrix anymore. Curr. Opin. Cell Biol., 13: 534-540.

15. Rahman, S.A., S. Nur, N. Abdul Wahab, A. Malek and S. Nurestri, 2013. In vitro morphological assessment of apoptosis induced by antiproliferative constituents from the rhizomes of Curcuma zedoaria. Evidence-Based Complementary Altern. Med., Vol. 2013, 10.1155/2013/257108

16. Levesque, R., 2007. SPSS Programming and Data Management: A Guide for SPSS and SAS Users. 4th Edn., SPSS Inc., Chicago.

17. Islam, F., H. Khatun, M. Khatun, S.M.M. Ali and J.A. Khanam, 2014a. Growth inhibition and apoptosis of Ehrlich ascites carcinoma cells by the methanol extract of Eucalyptus camaldulensis. Pharm. Biol., 52: 281-290.

18. Thomas, H.E., R. Darwiche, J.A. Corbett and T.W. Kay, 2002. Interleukin-1 plus γ-interferon-induced pancreatic ß-cell dysfunction is mediated by ß-cell nitric oxide production. Diabetes, 51: 311-316.

19. Cao, W., J.H. Peters, D. Nieman, M. Sharma, T. Watson and J. Yu, 2015. Macrophage subtype predicts lymph node metastasis in oesophageal adenocarcinoma and promotes cancer cell invasion in vitro. Br. J. Cancer, 113: 738-746.

20. Flatters, S.J.L., 2016.. Oxidative stress in the development, maintenance and resolution of paclitaxel-induced painful neuropathy. J. Mol. Catal., 1: 13-26.

21. Mamatha, G.C., T. Prabhakar, P. Naitik, V. Madhuri, K. Neelima and R. Erumalla, 2014. Antitumor activity and antioxidant status of Euphorbia Thymifolia Linn against Ehrlich ascites carcinoma in Swiss albino mice. World J. Pharmac. Res., 3: 853-864.

22. Warta, R. and C. Herold-Mende, 2017. Helping EGFR inhibition to block cancer. Nat. Neurosci., 20: 1035-1037.

23. Rivera, M., Y. Ramos, M. Rodriguez-Valentin, S. Lopez-Acevedo and L.A. Cubano *et al.*, 2017. Targeting multiple pro-apoptotic signaling pathways with curcumin in prostate cancer cells. PLoS One, Vol. 12, 10.1371 /journal.pone.0179587

24. Bell, R.A. and L.A. Megeney, 2017. Evolution of caspase-mediated cell death and differentiation: Twins separated at birth. Cell Death Differ., 24: 1359-1368.

25. Abbas, N.V., M.E. Shabana, F.M. Habib and A.A. Soliman, 2017. Histopathological and immune-histochemical study of matrix metalloproteinase-2 and matrix metalloproteinase-9 in breast carcinoma. J. Arab Soc. Med. Res., 12: 6-12.

26. Gupta, S.C., J.H. Kim, S. Prasad and B.B. Aggarwal, 2010. Regulation of survival, proliferation, invasion, angiogenesis and metastasis of tumor cells through modulation of inflammatory pathways by nutraceuticals. Canc Meta. Rev., 29: 405-434.

27. Li, Y.X., L. Run, T. Shi and Y.J. Zhang, 2017. CTRP9 regulates hypoxia-mediated human pulmonary artery smooth muscle cell proliferation, apoptosis and migration via TGF-ß1/ERK1/2 signaling pathway. Biochem. Biophys. Res. Commun., 490: 1319-1325.

28. Li, Y., D. Xing, Q. Chen and W.R. Chen, 2010. Enhancement of chemotherapeutic agent-induced apoptosis by inhibition of NF-?B using ursolic acid. Int. J. Cancer, 127: 462-473.

29. Man, S., W. Gao, Y. Zhang, L. Huang and C. Liu, 2010. Chemical study and medical application of saponins as anti-cancer agents. Fitoterapia, 7: 703-714.

30. Elsaid, F.G., 2013. The effect of seeds and fruit pulp of Adansonia digitata L. (Baobab) on ehrlich ascites carcinoma. Food Nutr. Sci., 4: 38-46.

31. Islam, F., S. Ghosh and J.A. Khanam, 2014b. Antiproliferative and hepatoprotective activity of metabolites from Corynebacterium xerosis against Ehrlich ascites carcinoma cells. Asian Pacific J. Trop. Biomed., 4: S284-S292.